Analysis of Noise Effects on the Nonlinear Dynamics of Synchronized Oscillators

Samuel Ver Hoeye, Almudena Suárez, *Senior Member, IEEE*, and Sergio Sancho

***Abstract*—The higher sensitivity to noise of nonlinear systems near the onset of instability is analyzed here. The analysis is particularized to synchronized oscillators, studying the influence of the proximity to Hopf and Saddle–Node bifurcations. The calculations are compared with former scaling relationships and with results from time-domain integration. The average shift of bifurcation points due to noise perturbations is also analyzed. Two examples are shown: a cubic-nonlinearity oscillator and a 5 GHz hybrid oscillator, for experimental verifications.**

***Index Terms*—Bifurcation, frequency conversion, Nyquist stability, oscillator noise, synchronization.**

I. Introduction

MANY authors [1]–[3] have observed the higher sensitivity to noise of nonlinear systems near bifurcations. The increase in the noise power, as the critical point is approached, is shown in [3], by making use of the conversion-matrix approach. Near a Hopf bifurcation (onset of a natural frequency [4]), the transient is a damped oscillation at the natural frequency, while, for instance, near a flip bifurcation (frequency division by two [4]), it is a damped oscillation of double period. The damping ratio is very low and, if noise is present in the system, the steady-state orbit is continuously perturbed, which makes observable the particular characteristics of the transient. This gives rise to noise amplification and bumps in the power spectrum or noisy precursors.

In the neighborhood of the bifurcation, complex nonlinear phenomena may also be observed. As an example, when two stable steady states of the unperturbed system coexist (for the same parameter values) and are close in the phase space, the solution may jump from one to another, under the noise influence (stochastic resonance). Another nonlinear phenomenon is the average shift of the bifurcation point due to the noise influence [5].

The analysis here is particularized to synchronized oscillators. Two examples are shown: a cubic nonlinearity oscillator and a 5 GHz hybrid oscillator.

II. Noisy Precursors

The Poincaré map of a nonautonomous circuit is obtained by sampling its steady state at integer multiples nT of the input generator period. Application of this technique to the cubic-nonlinearity oscillator in [4] provides the bifurcation diagram of Fig. 1(a), traced versus the input-generator frequency ω_g, for constant input-generator current $I_g = 20$ mA. The sampled variable is the voltage across the nonlinearity $v(nT)$. A noise-free circuit (black) and a white-noise current source (grey), with spectral density $|I_n|^2 = 10^{-12}$ A^2/Hz, have been considered. Fig. 1(b) shows the locus of the Floquet-multipliers [1] with the generator frequency as implicit parameter. The onset of the quasiperiodic regime is due to a saddle-node bifurcation at 1.58 MHz (one multiplier crossing the unity circle at $1e^{j0}$) and to a Hopf bifurcation at 1.33 MHz (two complex-conjugate multipliers crossing the circle at $1e^{\pm j\theta}$).

The multipliers are related to the Floquet exponents S_c through: $\mu_c = e^{s_c T} = e^{(\sigma_c + j\omega_c)T}$, with T the period of the steady-state solution. Note that there is not a univocal relationship between Floquet multipliers and exponents, since there is always a possible shift $\frac{2k\pi}{T} = k\,\omega_g$, with k integer. At a Hopf bifurcation, a new fundamental ω_a arises and $\omega_c = \omega_a + k\omega_g$. For a saddle-node bifurcation, there is no onset of new fundamentals and $\omega_c = 0 + k\omega_g$. Wiesenfeld [2] approximates the near-critical multipliers as $\mu_c \approx (1-\epsilon)e^j\theta$, ϵ being the distance to the border of the unit circle. A multiplier with magnitude close to one means a long lasting transient, due to the small value of σ_c. This slow transient, continuously interrupted by the noise perturbation, gives rise to an amplification of the noise spectrum, about the frequencies $k\omega_g$ (saddle node), or $k\omega_g \pm \omega_a$ (Hopf bifurcation).

For the analysis of the amplification effects, a deterministic tone $i_n(t) = I\cos(\omega t)$ can be considered. When the circuit operates close to a bifurcation, this tone introduces pairs of lines about $k\omega_g \pm \omega$, whose power increases [2] for a decrease of ϵ or/and a decrease of the frequency detuning $\Delta = (\omega - \omega_c)/\omega_g$, with ω_c the closest critical frequency. Here similar scaling properties to [2], have been obtained when using the stability margin M, instead of ϵ. This margin is calculated here as the minimum distance to the origin of the Nyquist plot. The power of the spectral lines $k\omega_g \pm \omega$ is approached by

$$S_k(\omega) = A_k \frac{I^2}{M^2 + \Delta^2} \tag{1}$$

where A_k is an unknown proportionality constant that has to be fitted. The Lorentzian lines obtained by sweeping ω in (1) become higher and narrower as the bifurcation point is approached. Clearly, the impact of precursors in the spectrum depends on the stability margin and its evolution versus the parameter. On the other hand, the scaling rule (1) fails in the immediate neighborhood of the bifurcation, since nonlinear

Manuscript received March 22, 2001; revised July 2, 2001. This work was supported by the FEDER Project 1FD97-0455-C02-01 (TIC). The review of this letter was arranged by Associate Editor Dr. Shigeo Kawasaki.

The authors are with the Departamento Ingeniería de Comunicaciones, University of Cantabria, Santander, Spain.

Publisher Item Identifier S 1531-1309(01)08084-9.

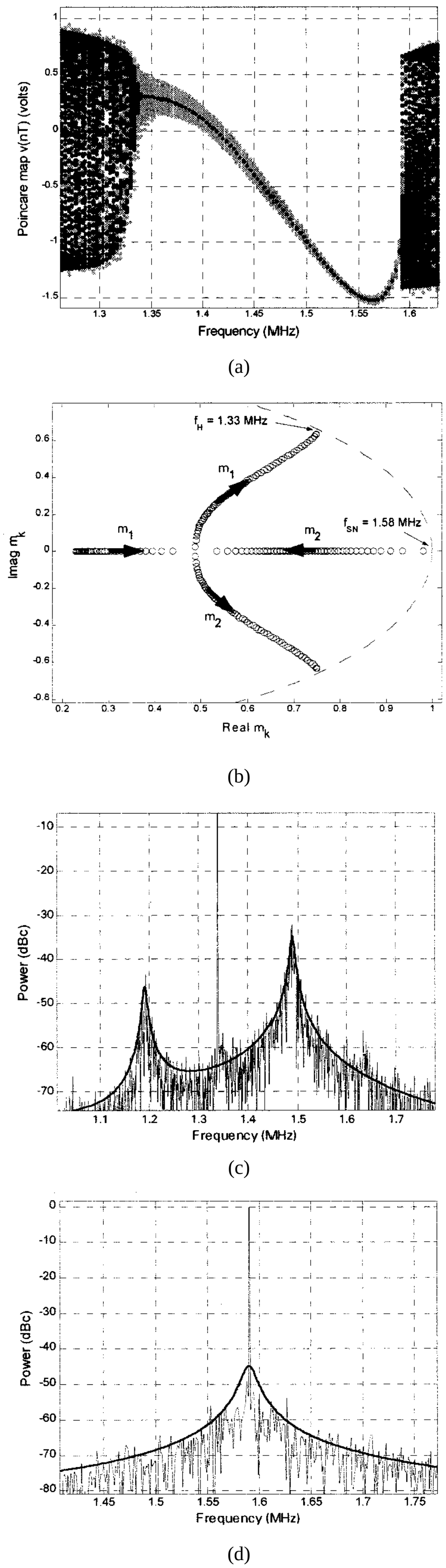

Fig. 1. Cubic nonlinearity oscillator [4], with $I_g = 20$ mA. (a) Poincaré map, sampling the voltage v, across the nonlinearity, (b) locus of Floquet multipliers m_k $(k = 1, 2)$, with the generator frequency as implicit parameter, (c) output spectrum for $f_g = 1.34$ MHz, close to the Hopf bifurcation, and (d) output spectrum for $f_g = 1.57$ MHz, close to the saddle-node bifurcation. In (c) and (d), the solid line is the frequency-domain simulation.

effects (due to the high power values) must be taken into account.

Frequency-domain linearization should enable the calculation of noisy precursors with the same restrictions as Floquet analysis [1]. The advantage over the time-domain techniques is the wider applicability to microwave circuits, due to the usually long transients of these circuits with respect to the signal period. Here, for the harmonic-balance analysis of the noisy precursors, an auxiliary generator AG, with negligible amplitude I, is introduced at the noise-source location $i_n(t) = \mathrm{Re}(\mathrm{I}e^{j\omega t})$. For a voltage output variable V and sweeping ω, this generator enables the calculation of the whole matrix relating $V(j, \pm 1)$ to $I(k, \pm 1)$ (conversion-matrix approach), where j, k (integers) are the harmonic indexes referring to ω_g and ± 1 are the indexes referring to ω. For Hopf bifurcations with $\omega_g/2 \leq \omega_a \leq \omega_g$, the spectrum bumps closest to ω_g are due to the amplification of input noise about ω_a and $2\omega_g - \omega_a$ (image frequency). Both in this case and for saddle-node bifurcations, the bumps are obtained, when sweeping ω, from the matrix terms relating $V(0, 1)$ and $V(2, -1)$, to both $I(0, 1)$ and $I(2, -1)$. In the noise spectrum calculation, the whole conversion matrix and the possible correlation of the noise sources must be taken into account.

The former technique has been applied for the analysis of the noisy precursors of the cubic-nonlinearity oscillator [4]. The results (solid line) are shown in Fig. 1(c) (close to the Hopf bifurcation) and Fig. 1(d) (close to the saddle-node bifurcation). Time-domain simulations have also been carried out, with an excellent agreement.

III. Stochastic Shift of the Stability Threshold

The presence of noise in a nonlinear circuit may give rise to an average shift of its stability thresholds. The shift depends on the amplitude and statistical properties of the noise perturbation. It is due to variations in the average magnitude of the Floquet multipliers, which may be decreased below unity or increased above unity [5]. To show this effect, the circuit bifurcation diagram is traced here by averaging the amplitude of one of the harmonic components for different time-domain realizations of the noise source (with the same power spectral density). This analysis, requiring time-domain simulations, has been applied to the cubic-nonlinearity oscillator. An intrinsic white-noise voltage source, in series with the nonlinearity, is initially considered, with spectral density 10^{-8} V^2/Hz. The resulting bifurcation diagram, close to the saddle-node (and averaging the first harmonic component), is shown in Fig. 2(a). As can be seen, noise reduces the bifurcation threshold.

In the frequency domain, the study of the bifurcation shift has been carried out versus a sinusoidal perturbation: $E\cos(\Omega t)$. A nonlinear analysis of the mixing steady state (with ω_g and Ω as fundamentals) is performed. Then the stability is analyzed through the Nyquist plot, applying [6]. The results have evidenced higher sensitivity for Ω close to ω_g. In Fig. 2(b), curve A shows the Nyquist plot for Ω very close to ω_g and $E = 10^{-4}$ V. The stability margin is decreased, in agreement with the time domain simulation. For low Ω, a high amplitude was necessary $E = 10^{-2}$ V, the effect being a stabilization of the synchronized solution (curve B).

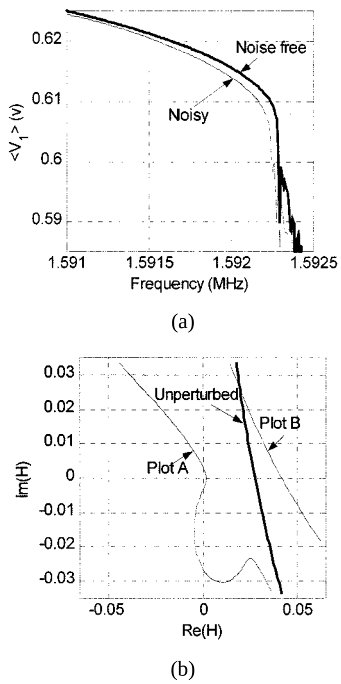

Fig. 2. Shift of the saddle-node bifurcation threshold. (a) Averaged bifurcation diagram for intrinsic white noise, with spectral density 10^{-8} V^2/Hz. The represented variable is the averaged first-harmonic component of the voltage across the nonlinearity and (b) Nyquist plot, using [6]. The function H is defined in [6]. Plot A: a sinusoidal tone close to ω_g, with amplitude $E = 10^{-4}$ V. Plot B: a low-frequency sinusoidal tone, with amplitude $E = 10^{-2}$ V.

IV. Experimental Results

As a final verification, a 5 GHz FET-based synchronized oscillator has been simulated and experimentally characterized. A Hopf-type bifurcation was obtained for $P_g = -6$ dBm and $f_g = 5.24$ GHz. In Fig. 3(a), the output-power spectrum has been determined (considering noise sources from the input generator and the oscillator itself) for two different input frequencies: $f_g = 5.19$ GHz and $f_g = 5.235$ GHz, to evidence the scaling properties of the precursors. One of the bumps is fixed at $f_a = 5$ GHz, while the other one (placed at $2f_g - f_a$) moves with the generator frequency. Noise power about the carrier is smaller than the precursor power. The experimental spectrum of Fig. 3(b) corresponds to $f_g = 5.24$ GHz, in the immediate neighborhood of the bifurcation point. The higher noise power about the carrier is due to nonlinear mixing effects, already present for this f_g value (extremely close to the bifurcation), which completely overwhelm the linear predictions.

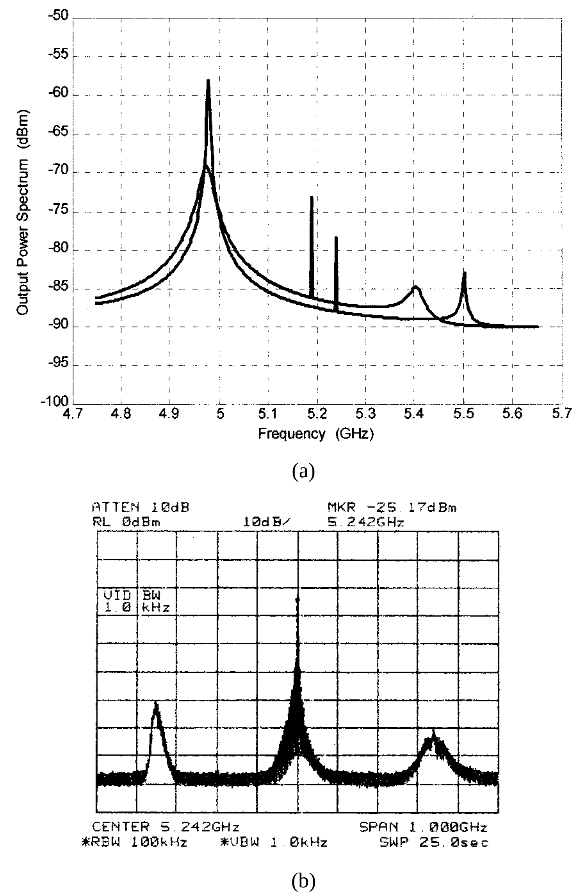

Fig. 3. Precursors of Hopf bifurcation for input power $P_g = -6$ dBm. (a) Simulation for $f_g = 5.19$ GHz and 5.235 GHz and (b) Measurement for $f_g = 5.24$ GHz, in the immediate neighborhood of the bifurcation. Nonlinear mixing effects are already present.

V. Conclusion

An analysis of the influence of noise on the nonlinear dynamics in the proximity to bifurcations has been carried out here. The formation of noisy precursors when approaching Hopf and saddle-node bifurcations, encountered in synchronized circuits, has been studied, comparing the predictions of time and frequency-domain analysis techniques. The stochastic shift of the bifurcation threshold has also been analyzed, through averaged bifurcation diagrams.

References

[1] K. Taihyun and E. H. Abed, "Closed-Loop monitoring systems for detecting incipient instability," in *Proc. 37th IEEE Conf. Decision Contr.l*, December 1998, pp. 3033–3039.
[2] K. Wiesenfeld, "Period doubling bifurcations: what good are they," in *Noise in Nonlinear Dynamical Systems*, F. Moss and P. Mc-Clintock, Eds. Cambridge, U.K.: Cambridge Univ. Press, 1989, vol. 2, pp. 145–178.
[3] V. Rizzoli, A. Costanzo, F. Mastri, and C. Cecchetti, "Harmonic-Balance optimization of microwave oscillators for electrical performance, steady-state stability, and near-carrier phase noise," in *1994 IEEE MTT-S Int. Microwave Symp. Dig.*, June 1994, pp. 1401–1404.
[4] A. Suárez, J. Morales, and R. Quéré, "Synchronization analysis of autonomous microwave circuits using new global-stability analysis tools," *IEEE Trans. Microwave Theory Tech.*, vol. 46, pp. 494–503, May 1998.
[5] M. Lücke, "Bifurcation behavior under modulated control parameters," in *Noise in Nonlinear Dynamical Systems*, F. Moss and P. Mc-Clintock, Eds. Cambridge, U.K.: Cambridge Univ. Press, 1989, vol. 2, pp. 100–144.
[6] A. Suárez, V. Iglesias, J. M. Collantes, J. Jugo, and J. L. Garcia, "Nonlinear stability analysis of microwave circuits using commercial software," *Electron. Lett.*, vol. 34, pp. 1333–1334, June 1998.